Schumann Resonances [1]

Janis Galejs

Applied Research Laboratory, Sylvania Electronic Systems, a Division of Sylvania Electric Products Inc.,

40 Sylvan Road, Waltham, Mass.   02154

This paper reviews the current work in the field of Schumann resonances and discusses the topics of waveforms and frequency estimates, resonance frequencies and Q factors, source distributions and noise spectra, diurnal and seasonal changes of power spectra, and variations of resonance frequencies. Observations of the above phenomena are correlated with theoretical considerations.

1. Introduction

The resonances in the spherical shell between the earth and ionosphere that are due to azimuthal waves have been considered in two recent survey papers [Galejs, 1964a; Wait, 1964a]. This work contains experimental data as well as the required theory. The basic theory of the resonances has been reviewed by Wait [1964b]. In the present summary the emphasis will be on correlation between measurements and available theory. There will be no extensive analytical developments, but frequent references will be made to literature.

Based on theoretical considerations, Schumann [1952a, b, 1957] postulated resonances of the earth-to-ionosphere cavity. Koenig [1958, 1959, 1961] obtained the first experimental indication of Schumann resonances by observing noise waveforms in the output of a narrow band amplifier. Detailed frequency spectra of this noise were first obtained by Balser and Wagner [1960]. Other measurements have been reported by Fournier [1960]; Benoit and Houri [1961, 1962]; Lokken et al. [1961, 1962]; Polk and Fitchen [1962]; Gendrin and Stefant [1962a]; Balser and Wagner [1962a, b, 1963]; Rycroft [1963]; Chapman and Jones [1964].

The fundamental theory of Schumann resonances [Schumann 1952a, b, 1957] is discussed in a book by Wait [1962]. Raemer [1961a, b] considers the observable noise spectra as the response of the earth-to-ionosphere cavity due to lightning flashes all over the world, but the homogeneous sharply bounded ionosphere model of Raemer introduces high losses, and he does not succeed in reproducing the spectral measurements of Balser and Wagner [1960]. Galejs [1961a, b] uses an isotropic ionosphere model of exponentially increasing conductivity which is based on measured or calculated characteristics of the lower ionosphere.

This model permits a close reproduction of the noise spectra measurements in the resonance region, and it also provides an agreement with measured ELF attenuation rates [Chapman and Macario, 1956; Jean et al., 1961].

Models of an anisotropic ionosphere are difficult to apply to the problem of earth-to-ionosphere cavity resonances because of the variations of the magnetic field vector along the surface of the earth. The propagation parameters can be estimated in the presence of a horizontal magnetic field component from the work of Galejs and Row [1964] and of Galejs [1964b]. The earth-to-ionosphere cavity resonances have been analyzed for a nonhomogeneous ionosphere in the presence of a radial (vertical) magnetic field by Thompson [1963] and Galejs [1965]. A thin-shell approximation of the ionosphere with a superimposed radial magnetic field has been considered by Wait [1964c]. Some other work of Wait [1963a, b], although intended for a different frequency range, can also be applied to the earth-to-ionosphere resonance problem in the presence of a radial magnetic field.

Additional references are available in the comprehensive bibliography by Brock-Nannestad [1962].

2. Waveforms and Frequency Estimates

In wide band recordings of atmospheric signals an ELF component or slow tail follows the initial VLF component of the transient [Hepburn and Pierce, 1953; Liebermann, 1956a, b; Tepley, 1959; Pierce, 1960]. An oscillatory structure of the signal becomes noticeable by passing it through a band-pass filter. An example of a noise recording in the output of a 2 to 30 c/s band-pass filter [Lokken, 1964, private communication] is shown in figure 1. The two horizontal magnetic field components have been observed simultaneously in Canada and in Antarctica. There is a correlation between the high intensity ELF noise bursts

observed at the various sites. A recording of one of the waveforms is shown in figure 2. The darkened areas indicate resonance frequencies around 8, 14, and 20 c/s. Noise waveforms in the 5 to 20 c/s band have been reported by Polk and Fitchen [1962] and Polk [1962]. Figure 3 shows sample recordings of the outputs of two coils the axes of which are oriented in the north to south (N–S) and east to west (E–W) directions. Frequency of these waveforms has been estimated by counting the cycles between the second markers shown on the records. The average frequency computed in this procedure should be higher
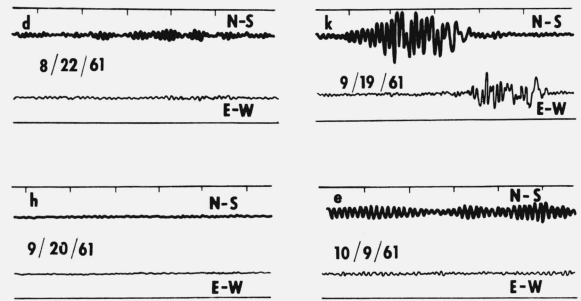

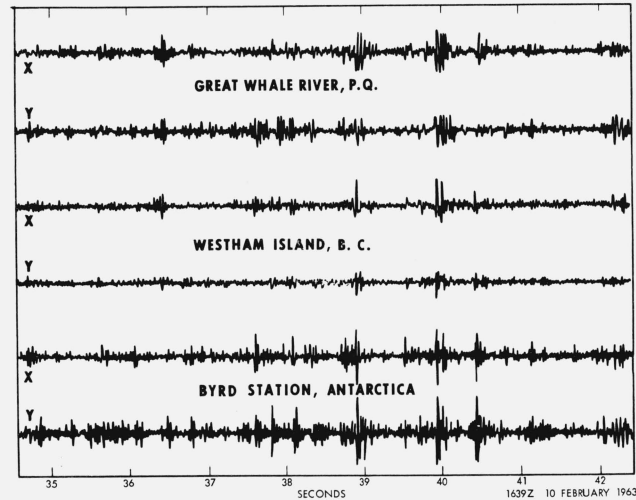FIGURE 3. *Noise recording in the 5 to 20 c/s band.*

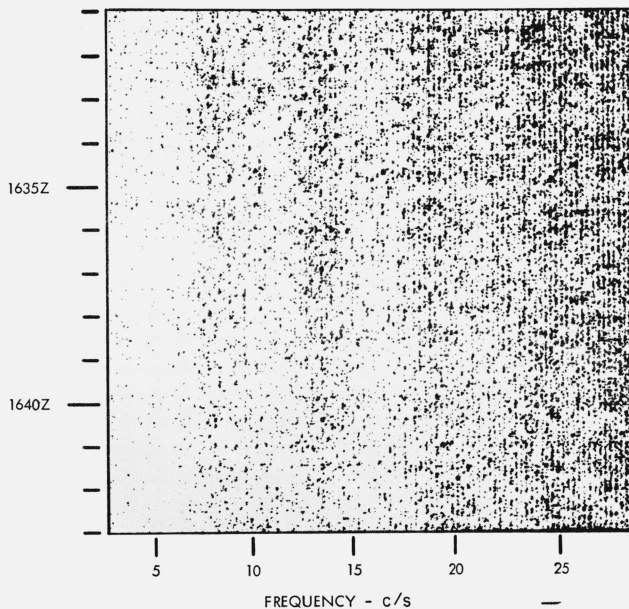FIGURE 1. *Noise recording in the 2 to 30 c/s band.*

FIGURE 2. *Recording of the noise waveform X of Westham Island, B.C.*

than the resonance frequencies of a spectral analysis [Galejs, 1962a, 1964a]. Noise recordings made simultaneously in Germany and in Rhode Island have been reported by Keefe, Polk, and Koenig [1964].

3. Resonance Frequencies and Q Factors

3.1. Definitions

A resonance frequency and Q factor may be determined from spectral measurements. Analytically it is also possible to compute the power spectrum of the noise waveform. However, it is more convenient to relate the resonance frequency and the Q factor to the analytically determined propagation parameters. The radial electrical field due to the vertical dipole excitation can be represented by

$$E_r = -\frac{iIds}{4\omega\epsilon ha^2} \frac{\nu(\nu+1)}{\sin \nu\pi} P_\nu(-\cos \theta) \qquad (1)$$

where

$$\nu(\nu+1) = (k_0 aS)^2. \qquad (2)$$

For a wave that propagates in the spherical shell between the earth and the ionosphere S is defined as the ratio of the complex wave number k to free space wave number $k_0(S = k/k_0)$. The real part of S can be seen to be inversely proportional to the phase velocity, and the imaginary part of S is proportional to the attenuation constant. This parameter S is determined from solving the appropriate boundary value problem of the earth, the air space and the chosen ionosphere model [Wait, 1962; Galejs, 1964a]. The resonance frequencies of the nth mode are determined from the minima of $\sin \nu\pi$ in (1) [Galejs, 1962a, 1964a] which gives

$$f_n \approx \frac{7.5 \sqrt{n(n+1)}}{\mathrm{Re}S}. \qquad (3)$$

Typical values of ReS are 1.4 to 1.2 for frequencies in the resonance region.

The cavity Q may be determined as a ratio between the stored energy and energy loss per cycle or simply by the width of the resonance curves. As shown in the appendix, in the present problem the electrically stored energy W_e differs from the magnetically stored energy W_h, and the Q definition should consider the sum of the average stored energies W_e and W_h. This expression for Q is

$$Q = \frac{(\text{Re}S)^2 + 1}{4\text{Re}S\,\text{Im}S}. \tag{4}$$

When considering only the magnetically stored energy Q is given by

$$Q = \frac{1}{2\,\text{Re}S\,\text{Im}S}. \tag{5}$$

For a given set of propagation parameters this will give a lower Q figure than (4). This expression has been used in the past work of Galejs [1961a, 1962a, b, 1964a]. Considering only the electrically stored energy gives

$$Q = \frac{\text{Re}S}{2\,\text{Im}S}. \tag{6}$$

The last expression can also be derived from the concept of complex resonance frequencies [Wait, 1964a] or by considering the half-power band width of the resonance curve. All three Q definitions yield the same results as $\text{Re}S$ approaches unity, but they will differ near the lower resonance frequency of the earth ionosphere cavity. Equation (4) will be used in the present calculation.

Experimentally determined Q values that are estimated from the half-power bandwidths of the resonance curves neglect the effects of adjacent resonances and of near-field noise that will tend to add to the background level. Hence, the half-power level is estimated too low, the apparent half-power bandwidth is larger and the estimated Q factor may be too low.

3.2. Characteristics of the Boundary

In the theoretical models that are advanced for explaining the resonance frequencies and the Q-factor measurements [Wait, 1962; Galejs, 1964a; Wait, 1964a] it is necessary to consider the boundary properties of the spherical shell.

In the frequency range of the resonances the displacement currents of ground are negligible and the ground conductivity $\sigma_g = 10^{-3}$ to 1 mho/m is much higher than the effective ionospheric conductivity σ_i that is estimated to be of the order of 10^{-7} to 10^{-6} mho/m. The ground conductivity σ_g may be assumed as infinite in the first approximation and only the ionospheric properties require a detailed analysis.

The ionosphere acts as an anisotropic conductor and for a z-directed magnetic field its conductivity

tensor is of the form

$$[\sigma] = \begin{bmatrix} \sigma_1 & -\sigma_2 & 0 \\ \sigma_2 & \sigma_1 & 0 \\ 0 & 0 & \sigma_0 \end{bmatrix}. \tag{7}$$

Equations for computing the conductivity components are available in literature [Galejs, 1964a and b] and typical conductivity profiles are shown in figure 4 but some uncertainties still apply to such models [Van-Zandt, 1964]. The above computations consider the ion effects, but assume the operating frequency to be zero. These profiles can be further approximated by straight lines through the lower ionosphere in the semilogarithmic plots of figure 4, which corresponds to an expoential height variation of the conductivity components. In a further simplification the anisotropy may be ignored ($\sigma_1 = \sigma_0$, $\sigma_2 = 0$). Even a simple one or two layer model can be assumed, such as shown in figure 5. These particular models have been used in past work by Raemer [1961a and b], Galejs [1962a and b], and by Chapman and Jones [1964]. In the isotropic exponential model the conductivity is given by

$$\sigma(z) = \sigma(z_0)\,\exp\,[\beta(z - z_0)] \tag{8}$$

where $z_0 = 60$ km and the day and night models are characterized by $\sigma(z_0) = 4.63 \times 10^{-8}$ mho/m and $\beta = 0.308$ km^{-1} and by $\sigma(z_0) = 6.5 \times 10^{-10}$ mho/m and $\beta = 0.44$ km^{-1}, respectively.
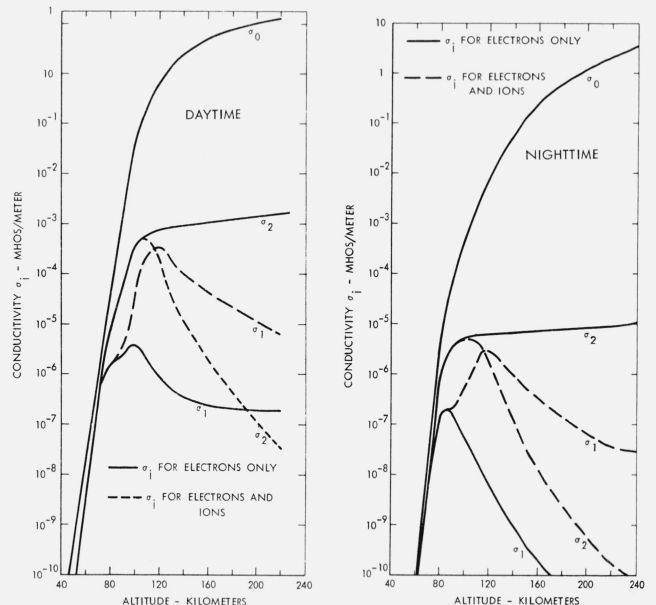

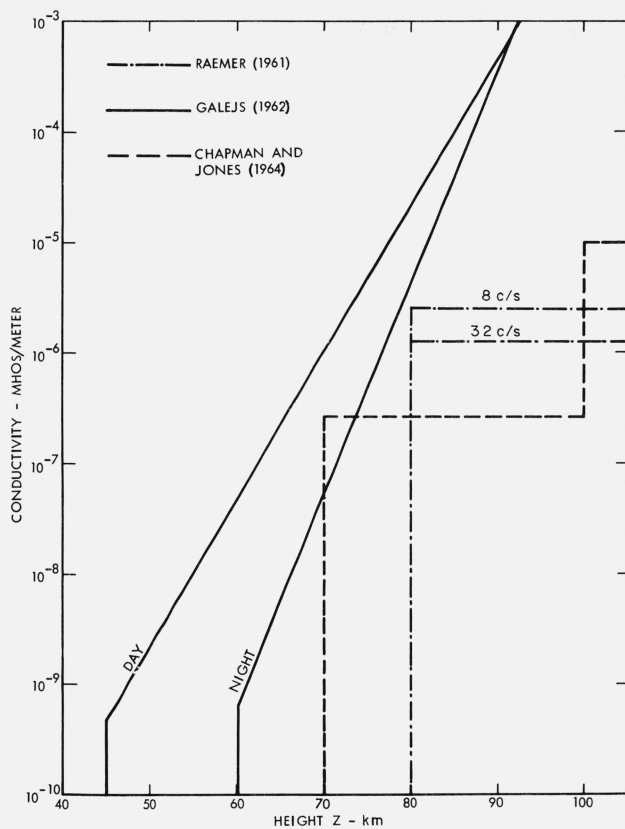FIGURE 4. *Components of the tensor conductivity* F = 0.

FIGURE 5. *Models of ionospheric conductivity.*

3.3. Single Layer Ionosphere

The single layer ionosphere model of Raemer [1961a and b] assumes the boundary height of the ionosphere to be constant, but the conductivity to change with frequency so as to obtain the correct resonant frequencies. However, the resulting Q factors are approximately two times lower than in measurements. The same difficulties are experienced with an ionosphere model of constant conductivity, but frequency dependent boundary height. Similar results are obtained by Madden [1961] with a conductivity of $\sigma = 1.8 \times 10^{-6}$ mho/m and the ionospheric boundary at $h = 80$ km. The deficiencies of a single layer ionosphere model are less pronounced if it is attempted to achieve only a partial match of the resonant frequencies, as seen from Wait [1964a]. However, the Q factors will be too low in particular at the higher resonance frequencies $(f \approx 30$ c/s).

Compressibility effects of the ionosphere have been considered by Seshadri [1965b] using the model of a perfectly conducting flat earth and a sharply bounded homogeneous isotropic and lossless ionosphere. The compressibility of the ionosphere does not affect the wave propagation below it for frequencies in the range of Schumann resonances and in the ELF band. However, the compressibility should be considered for waves that propagate inside the ionosphere [Seshadri, 1965a].

3.4. Two-Layer Ionosphere Models

Two-layer models give more accurate values of the resonance frequencies and of cavity Q or of the complex propagation parameter S. Two-layer and multilayer models have been discussed by Wait [1958, 1962]; Madden [1961]; Jean et al. [1961], and a particularly successful two-layer model has been constructed by Chapman and Jones [1964a, b]. This model, which is indicated in figure 5, has been applied in the frequency range of earth-to-ionosphere cavity resonances and also for frequencies up to 1 kc/s.

Such models are usually derived by trial and error procedures and they are difficult to correlate with continuous ionosphere profiles, such as shown in figure 4.

3.5. Models of Continuously Varying Ionosphere

The isotropic exponential model gives a reasonable approximation to the ionospheric conductivity versus height profile through the lower ionosphere layers, and the propagation parameters of the model can be determined from closed form expressions of the surface impedance [Galejs, 1961a, 1962a, b, 1964a]. Calculated resonance frequencies and Q factors that are based on (3), (4), and available values of S [Galejs, 1962a] are listed in tables I and II. Calculations are based on daytime or day and nighttime ionosphere models. The Q factors considered also the effects of cosmic ray ionization [Bourdeau et al., 1959] that give a nearly exponential conductivity versus height variation as indicated by Galejs [1962a]. Cosmic ray ionization decreases the effective Q figures, in particular for the lower frequencies. The calculated Q values are still somewhat higher than those estimated from experimental data.

TABLE 1

RESONANCE FREQUENCIES OF THE SPHERICAL SHELL BETWEEN THE EARTH AND IONOSPHERE

	n	1	2	3	4
RESONANCE FREQUENCY f_n IN C/S	LOSSLESS CAVITY	10.6	18.3	25.9	33.5
	DAYTIME WITH h = 45 KM	7.6	13.5	19.4	25.4
	AVERAGE DATA OF DAY WITH h = 45 KM AND OF NIGHT WITH h = 60 KM	8.05	14.25	20.5	26.8
	MEASUREMENTS	8	14.1	20.3	26.4

TABLE II

Q FACTORS OF EARTH-IONOSPHERE CAVITY RESONANCES

	f IN C/S	10	30	100
Q - FACTORS	DAY WITH h = 45 KM, NIGHT WITH h = 60 KM	8.5	7	6.7
	DAYTIME ONLY WITH h = 45 KM	6.5	5.4	5.2
	DAY WITH h = 45 KM, NIGHT WITH h = 60 KM, COSMIC RAY IONIZATION	5.5	6	6.4
	MEASUREMENTS	4	6	

3.6. Magnetic Field Effects

The magnetic field effects for a homogeneous sharply bounded ionosphere model have been discussed by Wait [1962] in a quasi-longitudinal approximation for a superimposed radial magnetic field and also for a transverse magnetic field (east-west or west-east propagation along the magnetic equator).

The propagation parameters have been determined by Galejs and Row [1964] and Galejs [1964a, 1964b] in the presence of a horizontal magnetic field. These data provide an indication of propagation characteristics of the waves near the magnetic equator, but they do not apply directly to the earth-ionosphere resonance problem, where the **H** vector is nearly horizontal only over a small surface portion of the earth.

The earth-ionosphere cavity resonance frequencies have been considered in the thesis of Thompson [1963] for a radial magnetic field. He uses a multilayer ionosphere model that approximates the continuous altitude variation of the conductivity tensor. The azimuthal field variation is expressed in terms of the Legendre polynomials $P_n(\cos\theta)$ for the nth mode. The wave equation has four different solutions for each of the ionosphere layers, but it has only two solutions for the space between the ionosphere and the perfectly conducting ground surface. The solution of the problem and the resonance condition for the mode n are obtained after multiplying a sequence of 4×4 matrices. In these computations the displacement currents of the ionosphere are neglected. The computed resonance frequencies are in agreement with measurements, but the Q values are in the range of 15 to 20, with the exception of nighttime anisotropic solutions, where $Q=7$ to 10. The lowering of the nighttime Q figures by the magnetic field has been attributed to wave penetration through the ionosphere and to energy thus escaping from the earth-ionosphere cavity.

Another solution to the problem of earth's ionosphere cavity resonance in the presence of a radial magnetic field is given by Galejs [1965]. The azimuthal field variation is expressed in terms of the Legendre functions $P_\nu(-\cos\theta)$, and the solution of the wave equation is set up so that the four solutions of the ionospheric layers where $\sigma > \omega\epsilon_0$ degenerate into two solutions for the lower ionospheric layers where $\sigma << \omega\epsilon_0$ and for free space. After computing the surface impedance at the lower boundary of the ionosphere, the propagation parameters are determined from the solutions of the modal equation for TM modes, although the coupling between TE and TM modes is considered in the processes of computing the surface impedance. Only the vertically polarized TM modes are assumed to propagate below the ionosphere. Such assumptions have been justified for a single layer ionosphere model at higher frequencies [Wait 1962, p. 269] and for a thin ionospheric shell also for frequencies in the resonance range [Wait, 1964c].

In the numerical calculations the anisotropic ionosphere models are those of figure 4 and further calculations are made for ionosphere models which consider electrons and ions at an operating frequency of 20 c/s, as indicated in figures 3 and 4 of Galejs [1964b]. In the isotropic ionosphere models σ_0 remains unaltered, $\sigma_1 = \sigma_0$, and $\sigma_2 \to 0$. The calculated resonance frequencies f_n are listed in table III. The isotropic day or night models exhibit too high resonance frequencies, but the average for the anisotropic day or night models gives nearly correct results, although the first resonance occurs near 7.7 c/s. At night the various anisotropic models give different results, while their results are nearly the same for daytime or for the isotropic models. The calculated Q factors are listed in table IV. At daytime the Q factors are lowered slightly due to anisotropy. The losses are principally due to absorption in the lower D region where the collision frequencies are high and the magnetic field has only small effects. At nighttime the anisotropy reduces the Q values drastically, and the ions have a considerable effect. For the isotropic models the energy remains below the ionosphere, the losses in the lower ionosphere are small and the Q values are high. For the anisotropic models some energy penetrates the ionosphere and escapes from the earth to ionosphere cavity. Hence the Q figure is low.

TABLE III

RESONANCE FREQUENCIES OF THE SPHERICAL SHELL BETWEEN THE EARTH AND IONOSPHERE IN THE PRESENCE OF A RADIAL MAGNETIC FIELD

IONOSPHERE MODEL		n 1	2	3	4
DAY, ANISOTROPIC		7.8	13.8	19.8	26
DAY, ISOTROPIC		8.1	14.2	20.4	26.6
NIGHT, ANISOTROPIC	EL.+ IONS F = 20	7.6	15.2	23.2	29.5
	EL.+ IONS F = 0	7.7	13.8	20.1	26.9
	EL. ONLY F = 0	7.8	14.1	20.7	27.8
NIGHT, ISOTROPIC		8.6	15.3	21.3	27.4
MEASUREMENTS		8	14.1	20.3	26.4

(RESONANCE FREQUENCY f_n IN C/S)

TABLE IV

Q-FACTORS OF EARTH-IONOSPHERE CAVITY RESONANCES IN THE PRESENCE OF A RADIAL MAGNETIC FIELD

IONOSPHERE MODEL		F 10	30
DAY, ANISOTROPIC		6.8	5.6
DAY, ISOTROPIC		8.3	7
NIGHT, ANISOTROPIC EL. + IONS F = 20		1.7	6.6
	EL. + IONS F = 0	2.0	2.7
	EL. ONLY F = 0	2.8	4.5
NIGHT, ISOTROPIC		8.8	9.3
MEASUREMENTS		4	6

(Q-FACTORS)

The previous calculations have assumed a constant radial magnetic field (S pole) all over the globe. A reversal of the static magnetic field (N pole) causes

negligible differences in the propagation parameters or in the values of f_n and Q. Hence a model using the average of the radial magnetic field may provide a first order estimate of the anisotropy effects. The present calculations assume the radial magnetic of the polar regions to be extended over the whole surface of the globe and the anisotropy effects should be too pronounced. The analytical results are highly dependent on the detailed structure of the nighttime anisotropic ionosphere, and further studies of it may be in order.

4. Source Distributions and Noise Spectra

Most of the ELF energy is of terrestrial origin and is caused by thunderstorm activity, although there are some high latitude events of an apparent extra-terrestrial origin. Such emissions of approximately 800 c/s have been detected near Kiruna, Sweden [Egeland, 1964] and of 14 to 17 c/s on Kerguelen Island in the Southern part of the Indian Ocean [Gendrin and Stephant, 1964, private communication]. The Spectran recording of the signals received at Kerguelen is shown in figure 6. The upper trace shows a normal signal with resonances near 8, 14, 20, and 25 c/s. There is an additional signal of 14 to 17 c/s on the two lower traces. When neglecting the presence of such extraneous signals the terrestrial noise spectra can be calculated after estimating the dipole moments of the sources and using propagation parameters that are appropriate to the selected ionosphere model.
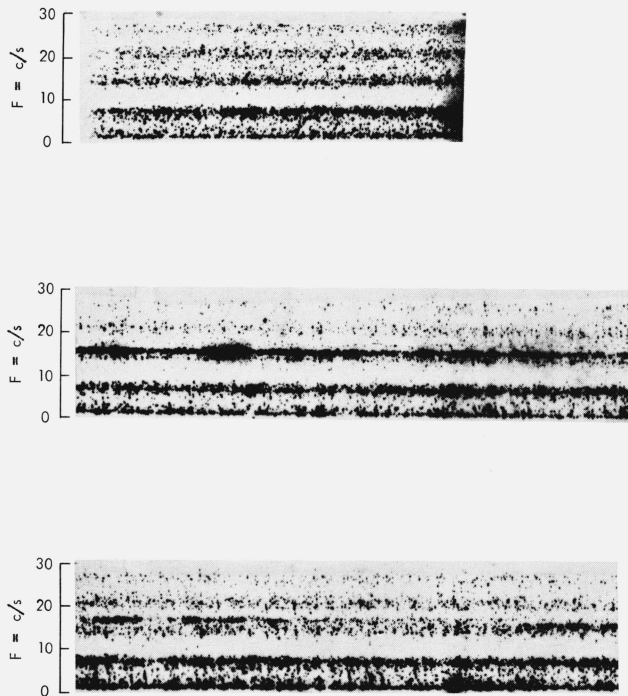
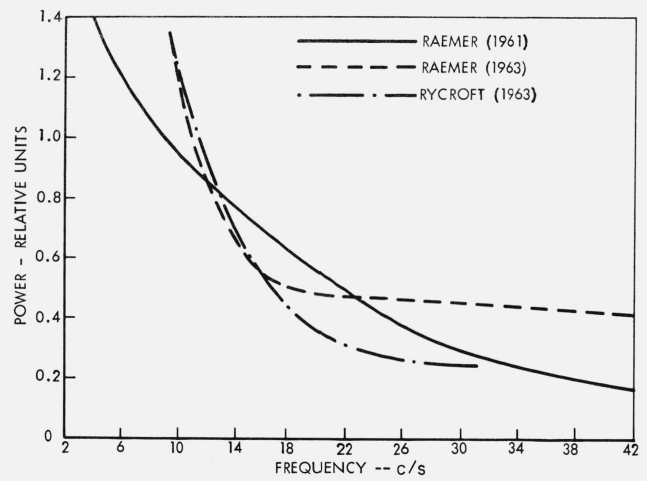FIGURE 6. *Spectran recordings of noise waveforms at Kerguelen Island.*

FIGURE 7. *Estimated lighting flash spectrum.*

Raemer [1961a, b] has estimated the power spectrum of the dipole moment in a median lightning flash Ids (or the first derivative of the electrostatic moment dM/dt) based on statistics of lightning strokes compiled by Williams [1959]. Later work of Raemer [1963 private communication] has lead to a revised estimate. These spectra are shown in figure 7. Pierce [1963] has computed the magnitude of the frequency spectra of the second derivative d^2M/dt^2, and Rycroft [1963] has calculated the frequency spectra of dM/dt using a similar representation of the lightning moments. The square of the frequency spectrum computed by Rycroft [1963] is also indicated in figure 7.

An equivalent power spectrum for the dipole moment of terrestrial noise sources has been deduced by Harris and Tanner [1962] from the measurements of Balser and Wagner [1960] by estimating the complex propagation constant within this frequency range in a "trial and error" approach. Harris and Tanner [1962] do not require an ionosphere model or any knowledge of lightning waveforms and their statistics for obtaining this equivalent power spectrum.

After determining the source spectra and the propagation parameters the power spectrum of the received noise may be computed from

$$G(i\omega) = \frac{g(i\omega)\,|\nu\,(\nu+1)|^2}{8(ak_0h)^2\,|\nu+\frac{1}{2}|\,[\cosh(2\pi\,\mathrm{Im}\,\nu)-\cos(2\pi\,\mathrm{Re}\,\nu)]}$$
$$\cdot\left\{\frac{\sinh\,[2\,\mathrm{Im}\,\nu\,(\pi-\theta)\,]}{(-\,\mathrm{Im}\,\nu)}\right.$$
$$\left.-\frac{\sin\,[(2\,\mathrm{Re}\,\nu+1)\,(\pi-\theta)-(\pi/2)\,]}{\mathrm{Re}\,\nu+\frac{1}{2}}\right\}\genfrac{}{}{0pt}{}{\theta_2}{\theta_1}, \quad (9)$$

where the ν is given by (2) and where the sources are assumed to be uniformly distributed in the θ interval of $\theta_1 < \theta < \theta_2$. The derivation of (9) starts from (1) and Legendre functions $P_\nu(-\cos\,\theta)$ are replaced by an asymptotic expansion. There are also equivalent spectral representations in terms of Legendre polynomials [Raemer, 1961a, b].
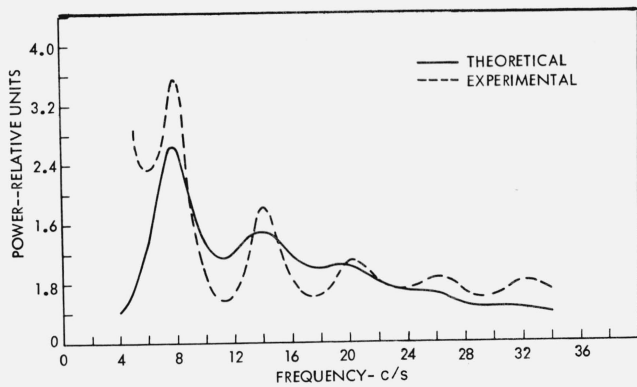
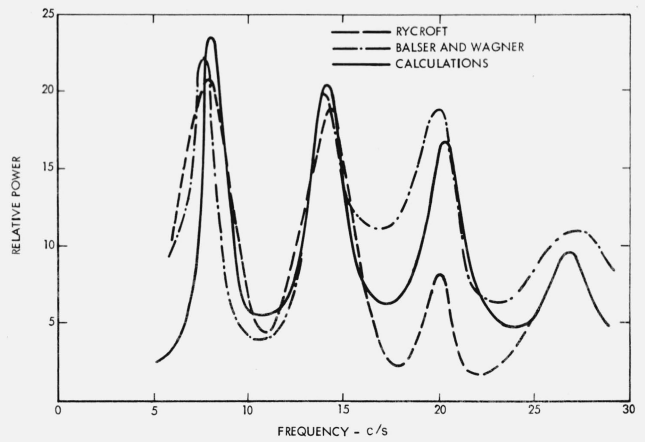FIGURE 8. *ELF Noise spectrum—effective ionospheric height assumed constant.*

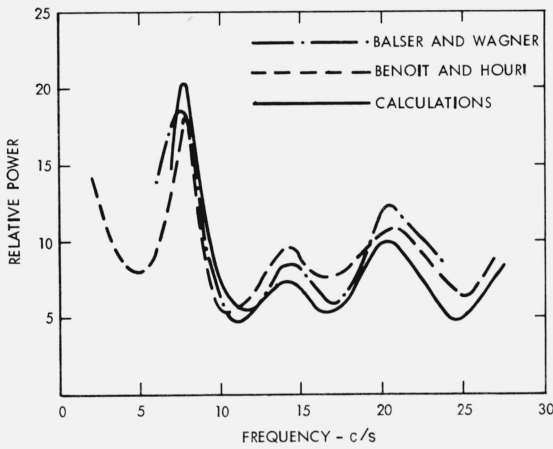FIGURE 10. *Noise spectrum for $47° \leq \theta \leq 128°$.*

FIGURE 9. *Noise spectrum for $38° \leq \theta \leq 72°$.*

FIGURE 11. *Diurnal variation of the resonance modes at Ipswich, Mass., February 1961 (vertical electric field), Chambon-la-Foret (near Paris) July 1962 and at Tromso (Norway) April 1962 (horizontal magnetic field).*

The noise spectrum of Raemer [1961b] has been used for computing the observed noise spectra in conjunction with a sharply bounded ionosphere model. This spectrum is shown in figure 8 and is seen to exhibit excessively damped higher resonance peaks.

The exponential ionosphere model [Galejs, 1961b, 1962a, 1964a] produces a better agreement with measurements as seen in figures 9 and 10. In this work propagation is assumed to be uniform around the surface of the earth and the propagation parameters represent the average of day and night conditions. The sources are assumed to be uniformly distributed over the θ interval indicated in the figures (θ is defined with respect to the observer).

5. Diurnal and Seasonal Changes of Power Spectra

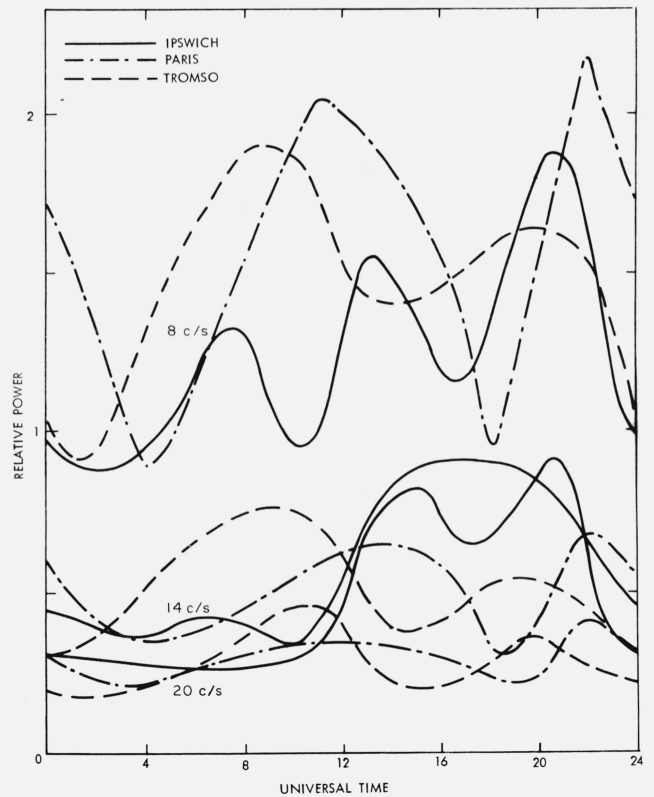Balser and Wagner [1962a] have recorded diurnal variations of measured noise spectra. Their measurements of the diurnal variations of the power level at the first three resonance frequencies are shown in figure 11 together with similar measurements by Gendrin and Stefant [1962a]. Diurnal variations of the fields near the two lower resonance frequencies have been measured at Kingston, R.I., by Polk, Huck, and Yu [1963, private communication]. The maxi-

1049

mum signal intensity occurs between 1500 and 1800 UT. In an amplitude versus time plot the signal peak is broader during summer than winter. Seasonal and diurnal variations of the noise power in the ELF frequency band below 35 c/s have been described by Wright [1963] without singling out the individual resonance modes. The measurements are made at Byrd Station, Antarctica (80°S, 120°W) and show peak intensities near 1000 UT during spring and summer and near 2300 UT during most of the year.

The gross features of the spectrum, such as the number of peaks and their approximate time of occurrence, may be explained qualitatively by noting areas of globe with particularly high thunderstorm activity and by measuring the polar angle θ from these source regions to the observation point. The vertical electric field E_r and the horizontal magnetic field H_ϕ of the mode n exhibit the θ dependence of

$$E_r \sim P_n(\cos\theta) \tag{10}$$

$$H_\phi \sim \frac{d}{d\theta} P_n(\cos\theta), \tag{11}$$

where $P_n(\cos\theta)$ is a Legendre polynomial of the order n. A particular geographical region will contribute to the measured values of E_r or H_ϕ in the mode n if the right hand sides of (10) or (11) are sizeable for those values of θ. Such considerations have been reported by Balser and Wagner [1962a] and Gendrin and Stefant [1962a].

More detailed calculations have been carried out by Abraham [1964, private communication; Galejs 1964a] who used available estimates of geographical distributions of the noise sources and who calculated the day and night propagation effects after expressing the fields as a sum of recirculating azimuthal waves.

In the expression for the electric field component E_r of (1), the Legendre function is replaced by the leading term of its asymptotic expansion. The function $\sin\nu\pi$ is expanded into

$$(\sin\nu\pi)^{-1} = -2i \sum_{n=0}^{\infty} e^{i(2n+1)\nu\pi} \tag{12}$$

which is valid for Im $\nu > 0$. This results in [Abraham, 1964, private communication]

$$E_r = \frac{Ids}{2\omega\epsilon ha^2} \frac{\nu(\nu+1)}{\sqrt{2\pi(\nu+\frac{1}{2})\sin\theta}} e^{i\frac{3\pi}{4}}$$

$$\sum_{n=0}^{\infty} \left\{ e^{i(\nu+\frac{1}{2})(\theta+2n\pi)-i2n\frac{\pi}{2}} + e^{i(\nu+\frac{1}{2})[2\pi(n+1)-\theta]-i(2n+1)\frac{\pi}{2}} \right\}. \tag{13}$$

The first term of the summation represents a wave which has traveled the direct distance from the source to the observation point (θ) plus n full circles around the sphere ($2n\pi$), while experiencing a phase shift of $(-\pi/2)$ radians at each traversal of the source point or its antipode. The other term of the summation represents a wave which has traveled toward the observation point across the antipode of the source $(2\pi - \theta)$ and has made furthermore n circles around the

sphere $(2n\pi)$ and has also experienced a phase shift of $(-\pi/2)$ radians at each traversal of the source point or its antipode. This physical interpretation of (13), which is equivalent to (1) for $\nu = $ const., permits a heuristic consideration of the ν differences between the day and night hemispheres. The multiplicative ν factors in front of the n summation are assumed to be constant and equal to $\bar{\nu}$ which is intermediate between the day and night ν values. The θ factors of the exponentials are replaced by integrals in order to account for the ν variation seen by the circular wave front as it propagates in the θ-direction with respect to the source. The amplitude changes at the day and night boundary can be also considered for each traveling wave by assuming that the energy of the wave remains constant after passing the day and night boundary. This results in decreased amplitudes for the larger ionospheric height of the night hemisphere. In the numerical work the surface of the earth was subdivided into 10° cells. Each cell had a constant surface density of noise sources but a variation was allowed from cell to cell. The plots of thunderstorm days over the world were used to set relative values of lightning activity for each of the cells, by assuming that the distribution of squared dipole moment per unit area is directly proportional to the thunderstorm day plots according to the Handbook of Geophysics [1960]. The diurnal variations were accounted for by a multiplicative factor in terms of local time at the source [Williams, 1959]. The final equation used in the spectrum calculations is similar to (9), although it is algebraically more involved [Abraham, 1964, private communication].

The diurnal variations of the noise power at the first three Schumann resonances have been computed using the exponential ionosphere model of figure 5 and are shown in figure 12. The calculations have disregarded the noise sources near the antipode where the usual asymptotic approximation of the Legendre functions is inaccurate. Figure 12 shows a qualitative agreement with the measurements of Balser and Wagner [1962a], that are shown in figure 11.

An example of seasonal power variations is shown in figure 13. It indicates a decreased noise power near the higher frequencies and/or during winter months.

Based on measurements at one location of the earth it is also possible to predict the noise levels at other locations using this procedure of noise spectrum calculations. The noise that is due to a worldwide distribution of thunderstorms depends on the frequency variation and also on the absolute value of the power spectrum of the mean dipole moment of the source $g(i\omega, \theta, \phi)$. The θ and ϕ dependence may be estimated from the thunderstorm frequency maps as was indicated before, which leaves the absolute value and the frequency dependence of $g(i\omega)$ as an unknown. Assuming that $g(i\omega)$ is the same for all noise sources, it may be determined by making the calculations to agree with measurements at one particular location. This gives a uniquely determined noise distribution over the surface of the earth and the accuracy of this model can be checked by com-
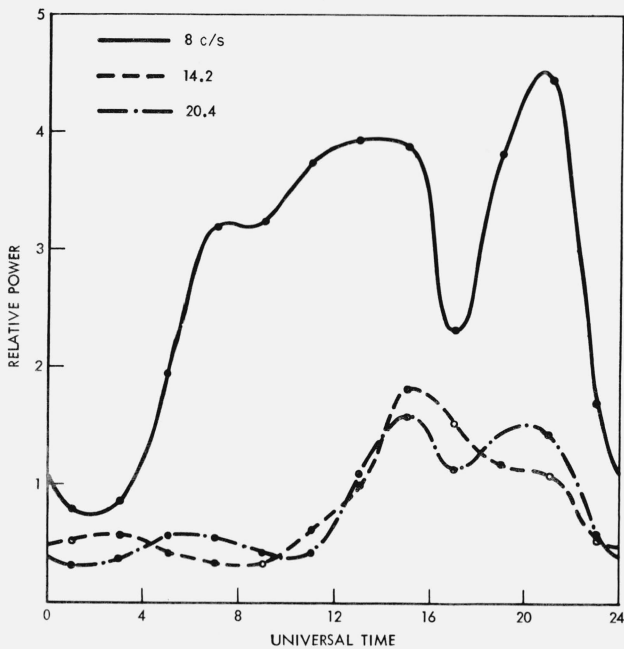
FIGURE 12. *Calculated diurnal variation of noise power at the peak of the resonance modes—wintertime—Boston, Mass.*
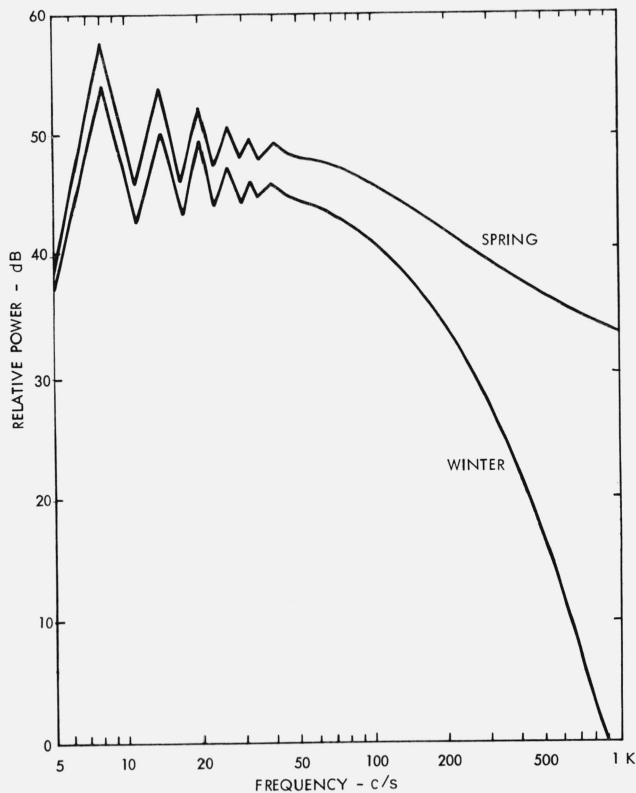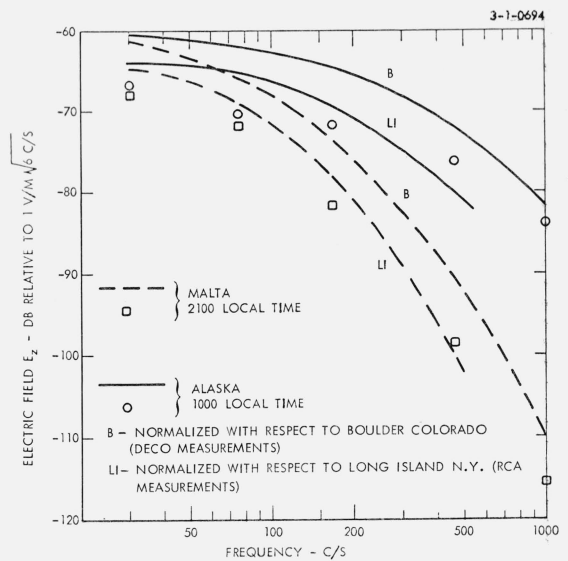

FIGURE 14. *Comparison of calculated field strength's data with July 1963 measurements by DECO and RCA.*

paring the calculations with measurements at other locations. In an example, measurements by DECO at Boulder, Colo., [Maxwell, 1963, private communication] and by RCA at Long Island, N.Y. [Powers, 1964, private communication], were used to determine $g(i\omega)$. The calculations by Abraham [1964, private communication] based on these values of $g(i\omega)$ have been compared with simultaneous measurements made in Malta and Alaska [Maxwell, 1963, private communication]. As seen from figure 14 the analytic curves agree in shape with the measurements, but the normalization with respect to Boulder gives somewhat higher predictions of the noise level. This may possibly be caused by summertime thunderstorm activity in the mountains near Boulder, Colo., that would give significant near-fields and a high estimate for the function $g(i\omega)$. The calculations are extended above the region of the earth-ionosphere cavity resonances to show that more significant noise level changes occur at higher frequencies.

In the calculations leading to figures 12 through 14 the day and night effects are considered most accurately if the day and night boundary is located symmetrically with respect to source (i.e., source at local noon or midnight). For nonsymmetrical day and night boundaries it is difficult to estimate the effects of wave front distortion. When neglecting such distortions (or assuming propagation strictly in the θ-direction), this method can account for $\nu(\theta)$ variations, which may be caused by ionosphere parameter changes or by changes of the static magnetic field along the surface of the earth. The assymptotic expansions of $P_\nu(-\cos\theta)$ used in (13) or (9) can be modified to increase their accuracy for observations near the source or its antipode [Abraham, 1965].

6. Variations of Resonance Frequencies

Diurnal frequency variations of the earth-ionosphere cavity modes have been reported by Balser and Wagner

FIGURE 13. *Calculated noise spectrum for local noon in northern hemisphere.*

[1962b], Gendrin and Stefant [1963], Rycroft [1963] and by Chapman and Jones [1964b]. The resonance frequencies vary by about ±0.2 to 0.3 c/s, but the changes are not simultaneous for the different modes; a low resonance frequency of one mode occurs simultaneously with a high frequency of a different mode.
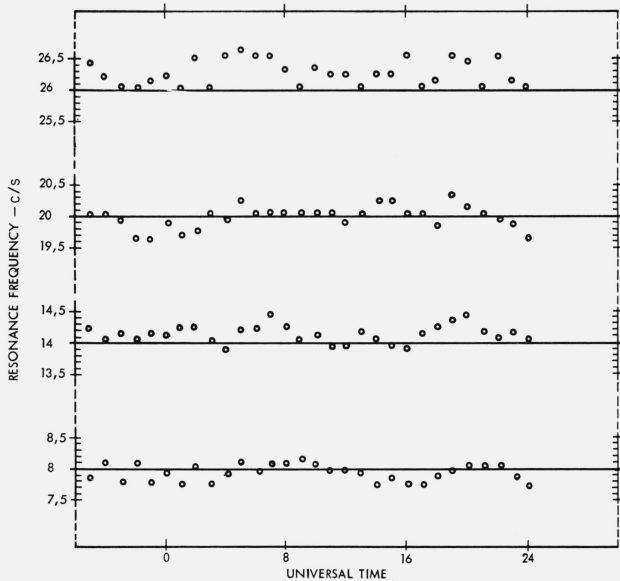

FIGURE 15. *Diurnal frequency variations measured by Gendrin and Stefant.*
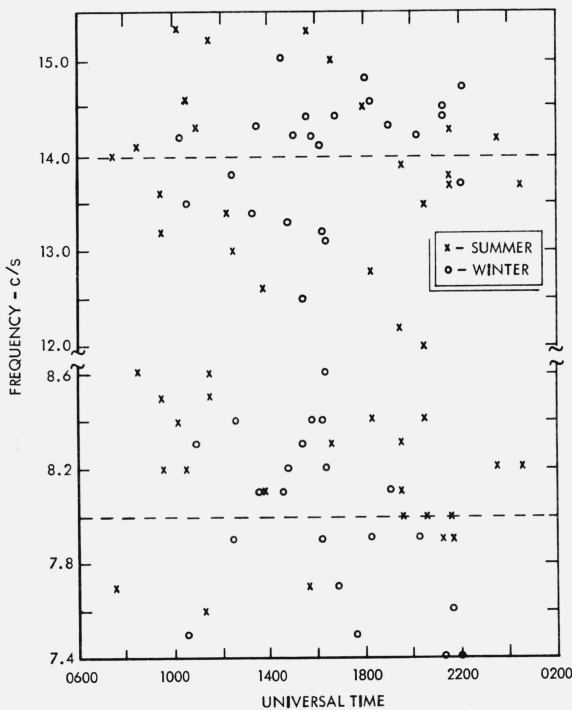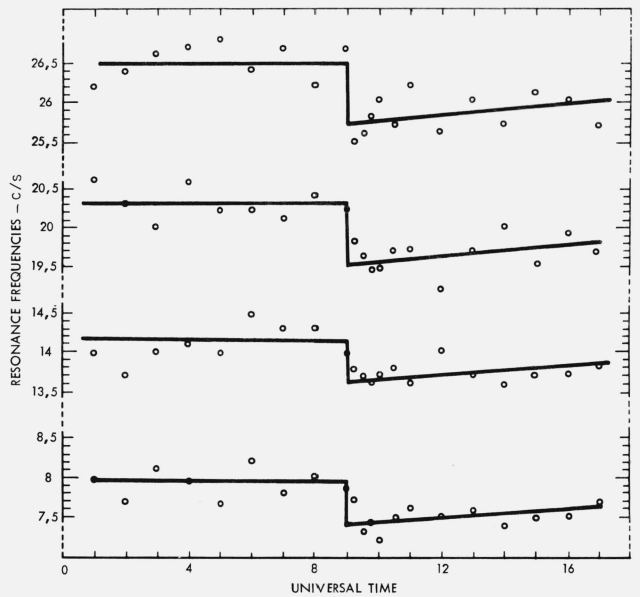

FIGURE 17. *Nuclear effects on earth-ionosphere cavity resonances.* Measurements by Gendrin and Stefant.

A high altitude nuclear explosion has been shown to affect the earth-to-ionosphere cavity resonances by simultaneously lowering all the resonance frequencies [Gendrin and Stefant, 1962a and b; Balser and Wagner, 1963]. Tepley et al., [1963] noted also an increase of signal strength for observations near the conjugate point of the explosion. The lowering of resonance frequency shown in figure 17 has been attributed to worldwide lowering of the effective ionosphere in a model of a single layer isotropic ionosphere [Gendrin and Stefant, 1962b]. The depression of the resonance frequency can be also explained by assuming an exponential daytime ionosphere to be effective around the globe [Row, 1964, private communication]. As an illustration the daytime resonance frequencies of table 1 compare with the measured resonance frequencies of figure 17. There are VLF observations [Zmuda et al, 1963] that can be explained by a lowering (or increasing electron density) of the D-region boundary. Brady et al., [1964] interpreted VLF diurnal phase shifts to show that some enhanced D-region ionization persists for several days following the event.

The lowering of the resonance frequency following a nuclear explosion has been attributed by Chapman and Jones [1964a] in their two-layer ionosphere model solely to a decreasing conductivity of the E-region.

After measuring a change of the resonance frequencies following a nuclear explosion, it is possible to advance simple ionosphere models for explaining a particular change. However, no attempt has been reported to predict resonance shifts for different nuclear yields and detonation altitudes. This rather complex problem requires a quantitative evaluation of the various nuclear mechanisms that may lead to ionosphere perturbations. If such information is

FIGURE 16. *Diurnal frequency variations measured by Rycroft.*

available, the computation of the resonance shifts is relatively simple. It would be also of interest to investigate the effects of sudden ionosphere disturbances (SID) and to discriminate between SID's and nuclear effects.

The resonant frequency changes can be considered more accurately with nonuniform models of the propagation geometry. A perturbation method [Wait, 1964b] or numerical techniques [Madden and Thompson, 1964] have been used for solving such problems.

Madden and Thompson [1964] compute the local surface impedance and propagation constant for a uniform cylindrical shell between the anisotropic ionosphere and the earth using matrix multiplication techniques. There is a smooth variation of the parameters between polar and equatorial regions and also between day and night hemispheres. These local surface impedances and propagation constants are assumed to characterize a spherical transmission line of nonuniform parameters. The resonance frequencies and Q factors are computed numerically using a lumped parameter approximation of the two-dimensional transmission line. This model has been applied to explain the diurnal frequency variations and also the frequency changes due to a nuclear explosion.

7. Areas of Future Work

There are numerous observations of earth-ionosphere cavity resonances and existing ionosphere and source models account for most observed characteristics like the resonance frequency, Q factors, shape of the noise spectra, and diurnal variations of the received power.

Future work appears to be required in a systematic study of diurnal and seasonal amplitude and frequency variations of resonances. These changes should also be correlated with ionospheric disturbances. The parameters of the nighttime ionosphere require also a future clarification. The variations of the ionosphere parameters and the variations of the magnetic field vector along the surface of the earth should be incorporated in future calculations [Wait, 1964b; Madden and Thompson, 1964]. Much work remains to be done for assessing nuclear effects on the earth ionosphere resonance and for discriminating between lower level nuclear and sudden ionospheric disturbances.

8. Appendix. Q Factors

The basic definition of the Q factor of a cavity with lossy walls is

$$\frac{1}{Q_i} = \frac{\int \int \mathbf{E} \times \mathbf{H}^* \cdot \mathbf{ds}}{\frac{\omega \epsilon_0}{2} \int \int \int \mathbf{E} \cdot \mathbf{E}^* dv + \frac{\omega \mu_0}{2} \int \int \int \mathbf{H} \cdot \mathbf{H}^* dv} \quad (14)$$

where the surface integral is extended over the cavity walls and the volume integral covers the inside of the cavity. The ground surface is assumed to be a perfect conductor and E_θ is related to H_ϕ at the ionospheric boundary by the surface impedance Z_s as $E_\theta = Z_s H_\phi$. However E_θ is assumed to be small relative to E_r for vertically polarized waves. Equation (14) is rewritten as

$$\frac{1}{Q_i} = \frac{2 \int \int \mathrm{Re} Z_s |H_\phi|^2 (a+h)^2 \sin \theta d\theta d\phi}{\omega \int \int \int [\epsilon_0 |E_r|^2 + \mu_0 |H_\phi|^2] r^2 dr \sin \theta d\theta d\phi} \quad (15)$$

$$\approx \frac{2 \mathrm{Re} Z_s}{\omega h} \frac{\int |H_\phi|^2 \sin \theta d\theta}{\int [\epsilon_0 |E_r|^2 + \mu_0 |H_\phi|^2] \sin \theta d\theta} \quad (16)$$

where a is the radius of earth, h is the ionospheric height and where the cavity is assumed to be uniform. For excitation by a radial electric dipole of moment Idr the field component E_r and H_ϕ follow from (21), (61), and (62) of Galejs [1964a] as

$$E_r = \frac{iIdr}{4\pi h \omega \epsilon a^2} \frac{n(n+1)(2n+1)}{D_n} P_n(\cos \theta) \quad (17)$$

$$H_\phi = -\frac{Idr}{4\pi h a} \frac{(2n+1)}{D_n} \frac{\partial}{\partial \theta} P_n(\cos \theta) \quad (18)$$

with $D_n = n(n+1) - \nu(\nu+1)$. Substituting (17) and (18) in (16) and evaluating the integrals gives

$$\frac{1}{Q_i} = \frac{2\mathrm{Re} Z_s}{\omega \mu_0 h \left[\frac{n(n+1)}{(k_0 a)^2} + 1 \right]} \quad (19)$$

where $k_0 = \omega \sqrt{\mu_0 \epsilon_0}$. From the approximate modal equation

$$S = \sqrt{1 + \frac{iZ_s}{\omega \mu_0 h}} \quad (20)$$

it follows that

$$2 \, \mathrm{Re} S \, \mathrm{Im} S = \frac{\mathrm{Re} Z_s}{\omega \mu_0 h} \cdot \quad (21)$$

Applying (21) and the resonance condition

$$n(n+1) \approx (k_0 a \, \mathrm{Re} S)^2 \quad (22)$$

(19) simplifies to

$$\frac{1}{Q_i} = \frac{4 \, \mathrm{Re} S \, \mathrm{Im} S}{(\mathrm{Re} S)^2 + 1} \quad (23)$$

which was listed as (4). When considering the differences of E_r, H_ϕ, Z_s, and h between the day and night hemispheres it follows that

$$\frac{1}{Q_i} \approx \frac{2[\text{Re}S \ \text{Im}S|_{day} + \text{Re}S \ \text{Im}S|_{night}]}{(\text{Re}S|_{avg})^2 + 1} . \quad (24)$$

The form (5) or (6) is obtained by neglecting the E integral or H integral, and by doubling the value of the H integral or E integral in (14).

9. References

Abraham, L. G. Jr., Aspects of the terrestrial ELF noise spectrum when near the source or its antipode, Radio Sci., J. Res. NBS **69D** (July 1965).

Balser, M., and C. A. Wagner (Nov. 1960), Observations of earth-ionosphere cavity resonances, Nature **188,** 638–641.

Balser, M., and C. A. Wagner (Feb. 1962a), Diurnal power variations of the earth-ionosphere cavity modes and their relationship to worldwide thunderstorm activity, J. Geophys. Res. **67,** No. 2, 619–625.

Balser, M., and C. A. Wagner (Sept. 1962b), On frequency variations of the earth-ionosphere cavity modes, J. Geophys. Res. **67,** No. 10, 4081–4083.

Balser, M., and C. A. Wagner (July 1, 1963), Effect of a high-altitude nuclear detonation on the earth-ionosphere cavity, J. Geophys. Res. **68,** No. 13, 4115–4118.

Benoit, R., and A. Houri (1961), Propagation of very-low-frequencies in the earth-ionosphere system, Ann. Geophys. (France) **17,** No. 4, 370–373.

Benoit, R., and A. Houri (Nov. 5, 1962), Power spectrum measurements of geophysical noise. Application to earth-to-ionosphere cavity, C. R. Acad. Sci. (France) **255,** 2496–2498.

Bourdeau, R. E., E. C. Whipple, and J. F. Clark (Oct. 1959), Analytic and Experimental Conductivity between the stratosphere and the ionosphere, J. Geophys. Res. **64,** 1363–1370.

Brady, A. H., D. D. Crombie, A. G. Jean, A. C. Murphy, and F. K. Stede (May 1, 1964), Long-lived effects in the D region after the high altitude nuclear explosion of 9 July 1962, J. Geophys. Res. **69,** 1921.

Brock-Nannestad, L. (Sept. 1962), Bibliography electromagnetic phenomena with special reference to ELF (1–3000 c/s) TR 10 Saclant, ASW Research Center, La Spezia, Italia.

Chapman, F. W., and D. L. Jones (May 16, 1964a), Earth-ionosphere cavity resonances and the propagation of extremely low frequency radio waves, Nature **202,** 654–657.

Chapman, F. W. and D. L. Jones, Observations of earth-ionosphere cavity resonances and their interpretation in terms of a two-layer ionosphere model, Radio Sci., J. Res. NBS **68D,** 1177–1185 (Nov. 1964b).

Chapman, F. W., and R. C. Macario (May 1956), Propagation of audio frequency radio waves to great distances, Nature **177,** 930–933.

Egeland, A. (1964a) ELF (500–1000 c/s) emissions at high latitude, Proc. NATO Advanced Study Institute on Natural Electromagnetic Phenomena Below 30 kc/s, Bad Homburg, West Germany, July–Aug. 1963, pp. 157–166 (Plenum Press, New York, N.Y.).

Fournier, H. (Aug. 17, 1960), Some aspects of the first high-frequency geomagnetic recordings obtained at Garchy, C. R. Acad. Sci. (France) **251,** No. 7, 962–964.

Galejs, J. (1961a), Terrestrial extremely-low-frequency noise spectrum in the presence of exponential ionospheric conductivity profiles, J. Geophys. Res. **66,** No. 9, 2787–2792.

Galejs, J. (Nov. 1961b), ELF waves in presence of exponential ionospheric conductivity profiles, IRE Trans. Ant. Prop. **AP-9,** 554–562.

Galejs, J. (July 1962a), A further note on terrestrial extremely-low frequency propagation in the presence of an isotropic ionosphere with an exponential conductivity-height profile, J. Geophys. Res. **67,** No. 7, 2715–2728.

Galejs, J. (1962b), Terrestrial extremely-low-frequency propagation in the presence of an isotropic ionosphere with an exponential conductivity height profile, Proc. International Conference on the Ionosphere, London, pp. 467–474 (Chapman and Hall).

Galejs, J. (1964a), Terrestrial extremely-low frequency propagation, Proc. NATO Advanced Study Institute on Natural Electromagnetic Phenomena Below 30 kc/s, Bad Homburg, West Germany, July–Aug. 1963, pp. 205–258 (Plenum Press, New York, N.Y.).

Galejs, J. (June 1964b), ELF and VLF waves below an inhomogeneous anisotropic ionosphere, Radio Sci. J. Res. NBS **68D,** No. 6, 693–707.

Galejs, J., and R. V. Row (Jan. 1964), Propagation of ELF waves below an inhomogeneous anisotropic ionosphere, IEEE Trans. Ant. Prop. **AP-12,** No. 1, 74–83.

Galejs, J., On the terrestrial propagation of ELF and VLF waves in the presence of a radial magnetic field, Radio Sci., J. Res. NBS **69D,** No. 5 (May 1965).

Gendrin, R., and R. Stefant (Sept. 1962a), Magnetic records between 0.2 and 30 c/s, AGARD Conference on Propagation of Radio Frequencies Below 300 kc/s, Munich, Germany.

Gendrin, R., and R. Stefant (1962b), Effects of the very high altitude nuclear explosion of the July 9, 1962 on the earth to ionosphere cavity resonances, experimental results and interpretation, C. R. Acad. Sci. **255,** 2273–2275 and 2493–2495.

Handbook of Geophysics (1960), USAF Air Research and Development Command, Airforce Cambridge Research Center (Macmillan Co., New York, N.Y.).

Harris, F. B., Jr., and R. L. Tanner (1962), A method for determination of lower ionosphere properties by means of field measurements on sferics, J. Res. NBS **66D** (Radio Prop.), No. 4, 463–478.

Hepburn, F., and E. T. Pierce (May 9, 1953), Atmospherics with very-low-frequency components, Nature (GB) **171,** 837–838.

Jean, A. G., Jr., and A. C. Murphys, J. R. Wait, and D. F. Wasmundt (1961), Propagation attenuation rates at ELF, J. Res NBS **65D** (Radio Prop.), No. 5, 475–479.

Keefe, T. J., C. Polk, and H. L. Koenig (1964), Results of simultaneous ELF measurements at Brannenburg (Germany) and Kingston, R.I., ULF Symposium, Boulder, Colo. Aug. 17–20, 1964.

Koenig, H. (Dec. 1958), Atmospherics geringster frequenzen, Dissertation an der Technischen Hochschule München.

Koenig, H. (July 1959), Atmospherics geringster frequenzen, Z. Angew. Phys. **11,** No. 7, 264–274.

Koenig, H., E. Haine, and C. H. Antoniadis (Aug. 1961), Messung von 'atmospherics' geringster frequenzen in Bonn, Z. Angew. Phys. **13,** No. 8, 364–367.

Liebermann, L. (Dec. 1956a), Extremely-low-frequency electromagnetic waves: I. Reception from lightning, J. Appl. Phys. **27,** No. 12, 1473–1476.

Liebermann, L. (Dec. 1956b), Extremely-low-frequency electromagnetic waves: II. Propagation properties, J. Appl. Phys. **27,** No. 12, 1477–1483.

Lokken, J. E., J. A. Schand, and C. S. Wright (1962), A note on the classification of geomagnetic signals below 30 c/s, Can. J. Phys. **40,** 1000–1009.

Madden, T. R. (1961), An analysis of the earth-ionosphere electromagnetic resonances, unpublished class notes for MIT course 12.88, April 24.

Madden, T. Rand, W. Thompson, Low-frequency electromagnetic oscillations of the earth-ionosphere cavity, Report on Project NRL 371–401, Geophysics Laboratory, MIT, Cambridge, Mass. (Sept. 22, 1964). Also Rev. Geophys. **3,** No. 2 (May 1965).

Pierce, E. T. (July–Aug. 1960), Some ELF phenomena, J. Res. NBS **64D** (Radio Prop.), No. 4, 383–386.

Pierce, E. T. (July 1, 1963), Excitation of earth-ionosphere cavity resonances by lightning flashes, J. Geophys. Res. **68,** No. 13, 4125–4127.

Polk, C., and F. Fitchen (May–June 1962), Schumann resonances of the earth-ionosphere cavity—extremely low frequency reception at Kingston, R.I., J. Res. NBS **66D** (Radio Prop.), No. 3, 313–318.

Polk, C. (1962), ELF propagation and the earth-ionosphere resonant cavity, paper presented at the meeting of the Ionospheric Research Committee of AGARD in Munich, West Germany, Sept. 17–21, 1962.

Raemer, H. R. (1961a), On the extremely-low-frequency spectrum of earth-ionosphere cavity response to electric storms, J. Geophys. Res. **66,** No. 5, 1580–1583.

Raemer, H. R. (Nov.–Dec. 1961b), On the spectrum of terrestrial radio noise at extremely low frequencies, J. Res. NBS **65D** (Radio Prop.), No. 6, 581–594.

Rycroft, M. J. (Dec. 1963), Low frequency disturbances of natural origin of the electric and magnetic fields of the earth, Ph.D. Thesis, University of Cambridge.

Schumann, W. O. (1952a), Über die strahlungslosen Eigenschwingungen einer leitenden Kugel, die von einer Luftschicht und einer Ionosphärenhülle umgeben ist, Z. Naturforsch, **72,** 149–154.

Schumann, W. O. (1952b), Über die Dämpfung der elektromagnetischen Eigenschwingungen des Systems Erde-Luft-Ionosphäre, Z. Naturforsch **72,** 250–252.

Schumann, W. O. (Aug. 1957), Elektrische Eigenschwingungen des Hohlraumes Erde-Luft-Ionosphäre, Z. Angew. Phys. **9,** 373–378.

Seshadri, S. R., Radiation from electromagnetic sources in a plasma, IEEE Transactions on Antennas and Prop. **AP-13,** No. 1, 79–88 (Jan. 1965a).

Seshadri, S. R. (March 1965b), VLF propagation in a sharply bounded, compressible isotropic ionosphere, IEEE Trans. Ant. Prop. **AP-13,** No. 2, 311–317.

Tepley, L. R. (Dec. 1959), A comparison of sferics as observed in the very-low-frequency and extremely-low-frequency bands, J. Geophys. Res. **64,** No. 12, 2315–2329.

Tepley, L., R. C. Wentworth, K. G. Lambert, H. V. Prentiss, K. D. Amundsen and D. R. Hillendahl (26 Dec. 1963), Sub ELF geomagnetic fluctuations, III final report Contract AF 19(628)–462, Lockheed Missile and Space Co., Palo Alto, Calif.

Thompson, W. B. (Feb. 1963), A layered model approach to the earth-ionosphere cavity resonance problem, Ph.D. Thesis, Department of Geology and Geophysics, MIT.

VanZandt, T. E. (1964), Ionosphere, ULF Symposium, Boulder, Colo., Aug. 17–20.

Wait, J. R. (March 1958), Extension to mode theory of VLF propagation, J. Geophys. Res. **63,** 125–135.

Wait, J. R. (1962), Electromagnetic waves in stratified media (Macmillan Co., New York, N.Y.).

Wait, J. R. (Feb. 1963a), The mode theory of VLF radio propagation for a spherical earth and a concentric anisotropic ionosphere, Can. J. Phys. **41,** 299–315.

Wait, J. R. (May–June 1963b), Concerning solutions of the VLF mode problem for an anisotropic curved ionosphere, J. Res. NBS **67D** (Radio Prop.), No. 3, 297–302.

Wait, J. R. (April 1964a), On the theory of Schumann resonances in the earth-ionosphere cavity, Can. J. Phys. **42,** 575–582.

Wait, J. R. (1964b), Earth-ionosphere cavity resonances and the propagation of ELF radio waves, ULF Symposium, Boulder, Colo., Aug. 17–20. Also Radio Sci. J. NBS **69D,** No. 8.

Wait, J. R. (1964c), Cavity resonances for a spherical earth with a concentric anisotropic shell (private communication).

Wait, J. R. (1964d), A note on the Schumann problem for nonuniform boundaries (private communication).

Williams, J. C. (May 1959), Thunderstorms and VLF radio noise, Ph.D. Thesis, Harvard University, Division of Engineering and Applied Physics.

C. S. Wright (July–Aug. 1963), Conjugate relations of micropulsations and other ionospheric phenomena, NATO Advanced Study Institute on Natural Electromagnetic Phenomena Below 30 kc/s, Bad Homburg, Germany.

Zmuda, A. J., B. W. Shaw, and C. R. Haave (Feb. 1, 1963), VLF disturbances and the high-altitude nuclear explosion of July 9, 1962, J. Geophys. Res. **68,** No. 3, 745–758.

(Paper 69D8–538)